Petrovic et al., http://www.jcb.org/cgi/content/full/jcb.201002070/DC1

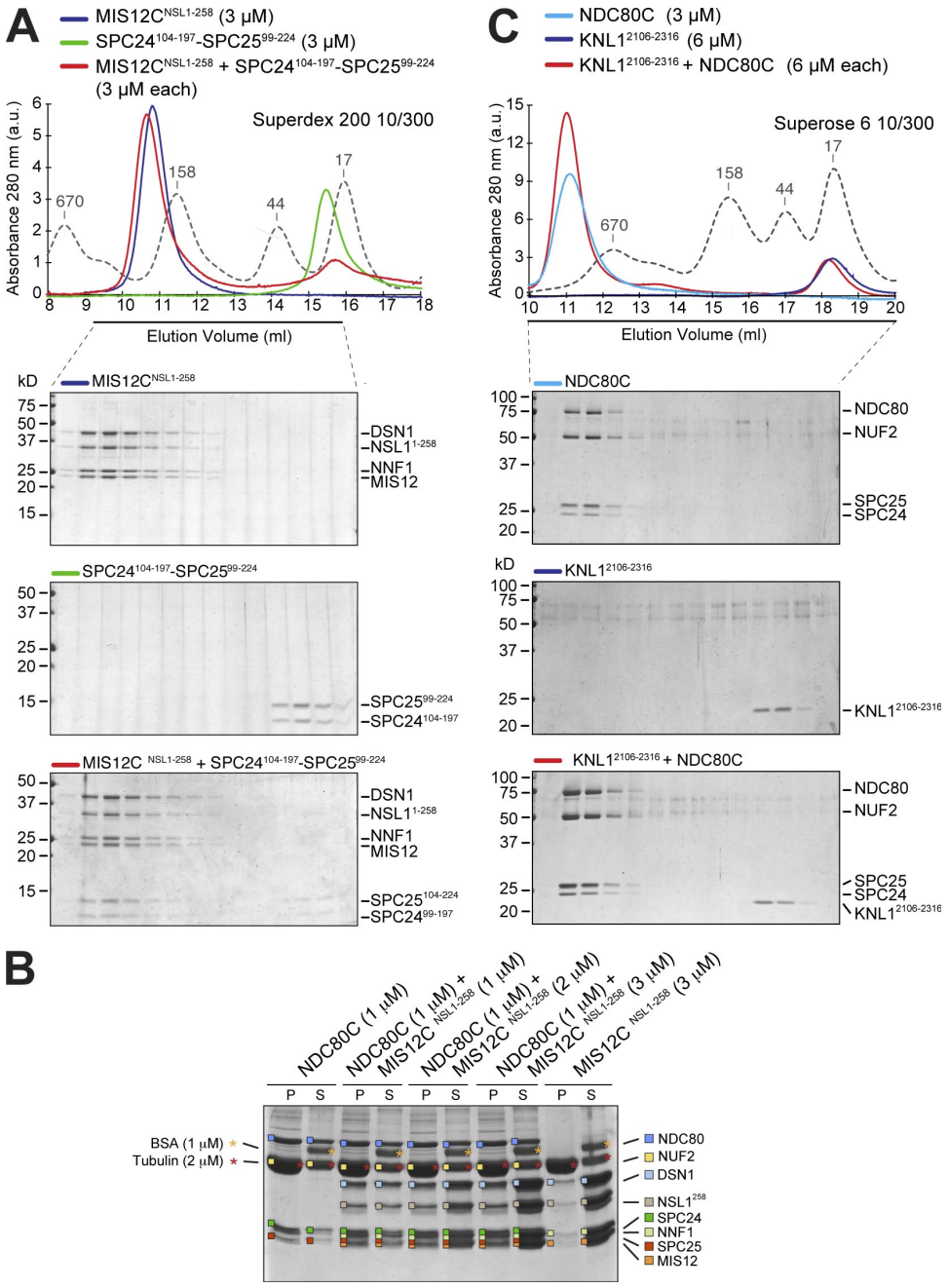

Figure S1. **Additional properties of the MIS12C–NDC80C–KNL1 interaction.** (A) Size-exclusion chromatography elution profiles and SDS-PAGE analysis of MIS12C$^{NSL1-258}$ (top), SPC24$^{104–197}$–SPC25$^{99–224}$ (middle), and their stoichiometric combination (bottom). A stoichiometric MIS12C$^{NSL1-258}$–SPC24$^{104–197}$–SPC25$^{99–224}$ complex forms, showing that the short SPC24–SPC25 construct is sufficient to bind MIS12C. (B) Pellet (P) and supernatant (S) partitions of taxol-stabilized microtubule binding assays performed with growing concentrations of MIS12C. MIS12C does not cosediment with microtubules, nor does it increase the affinity of NDC80C for microtubules. At the concentrations of NDC80C and salt used in this assay, ~60% of NDC80C is found in the microtubule pellet. The same ratio of NDC80C in the pellet and supernatant fractions is observed in the presence of MIS12C, suggesting that the latter does not increase the binding affinity of NDC80C for microtubules. (C) Size-exclusion chromatography elution profiles and SDS-PAGE analysis of recombinant NDC80C expressed in, and purified from, insect cells (top), KNL1$^{2106–2316}$ (middle), and their stoichiometric combination (bottom). No binding was observed. (A and C) Dashed gray lines and numbers indicate elution markers in the size-exclusion chromatography experiments and their molecular masses (in kilodaltons), respectively.

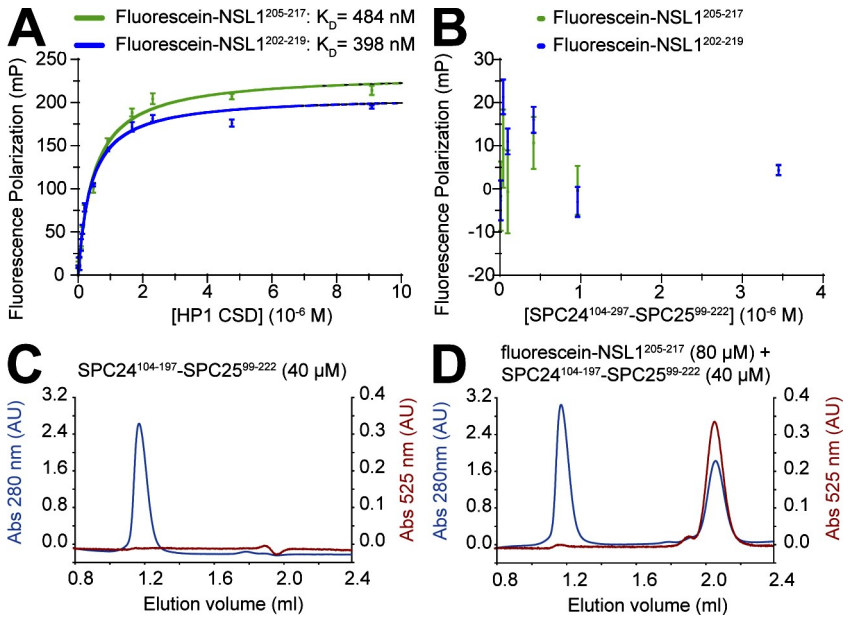

Figure S2. **NDC80C does not bind tightly to the PVIHL motif of NSL1.** (A) Fluorescence anisotropy measurements with 10 nM of fluoresceinated NSL1$^{205–217}$ or NSL1$^{202–219}$ peptides and varying concentrations of the chromoshadow domain (CSD) of HP1-α. Curves were fitted as described in Materials and methods. The derived dissociation constants are indicated. (B) No significant change in fluorescence anisotropy was observed when the same experiment was performed with the SPC24$^{104–197}$–SPC25$^{99–224}$ construct, which is shown in Fig. S1 A to be able to bind MIS12C. We conclude that a short region encompassing the PVIHL motif in insufficient for MIS12C binding by SPC24–SPC25. Error bars indicate standard deviations from three experiments. (C) Elution profile from a size-exclusion chromatography Superdex 75 PC 3.2/30 column of SPC24$^{104–197}$–SPC25$^{99–224}$. The blue and red traces report absorbance (Abs) at 280 nm and 525 nm, respectively. (D) The SPC24$^{104–197}$–SPC25$^{99–224}$ construct does not coelute with the fluorescein-NSL1$^{205–217}$ peptide, suggesting that this region of NSL1 is insufficient for high-affinity binding to NDC80C. AU, arbitrary unit.

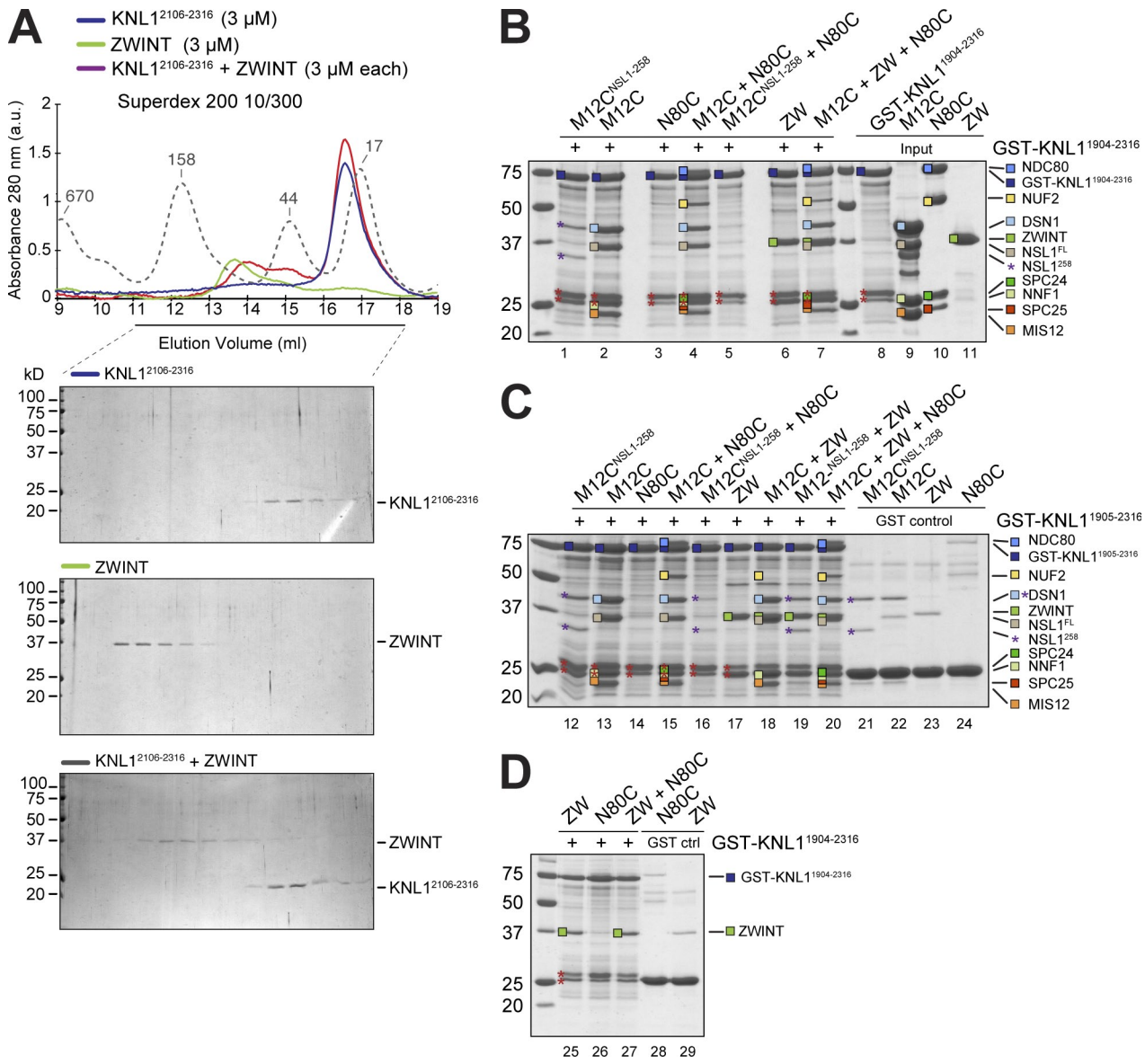

Figure S3. **Additional characterization of the role of ZWINT.** (A) Size-exclusion chromatography elution profiles and SDS-PAGE analysis of KNL1$^{2106–2316}$ (top), ZWINT (middle), and their stoichiometric combination (bottom). No binding was observed. The dashed gray line and numbers indicate elution markers in the size-exclusion chromatography experiments and their molecular masses (in kilodaltons), respectively. (B) A GST-KNL1$^{1904–2316}$ fusion protein was used as an affinity bate on glutathione Sepharose beads. This construct was then incubated with the input proteins shown on the right (except for the MIS12C$^{NSL1-258}$ construct, which is shown in Fig. 1 B). The red asterisks mark two bands that copurify with GST-KNL1$^{1904–2316}$ on the glutathione Sepharose beads. No binding to MIS12C$^{NSL1-258}$ was observed (lane 1). MIS12C binds GST-KNL1$^{1904–2316}$ (lane 2). Colored squares on the left of a band are added to simplify the interpretation. NDC80C does not bind GST-KNL1$^{1904–2316}$ directly (lane 3). NDC80C binds GST-KNL1$^{1904–2316}$ in the presence of MIS12C (lane 4) but not MIS12C$^{NSL1-258}$ (lane 5). ZWINT (ZW) binds GST-KNL1$^{1904–2316}$ (lane 6). ZWINT, MIS12C, and NDC80C form a supramolecular complex on GST-KNL1$^{1904–2316}$ (lane 7). (C) Lanes 12–17 and 20 are equivalent to lanes 1–6 and 7 of panel B, respectively. MIS12C and ZWINT bind GST-KNL1$^{1904–2316}$ (lane 18). ZWINT does not allow binding of MIS12C$^{NSL1-258}$ to GST-KNL1$^{1904–2316}$ (lane 19). The purple asterisks indicate background levels of MIS12C$^{NSL1-258}$ binding to GST, shown in lane 21. (D) ZWINT binds GST-KNL1$^{1904–2316}$ (lane 25). NDC80C does not bind GST-KNL1$^{1904–2316}$ (lane 26). The presence of ZWINT does not allow NDC80C to bind GST-KNL1$^{1904–2316}$ (lane 27). ctrl, control.

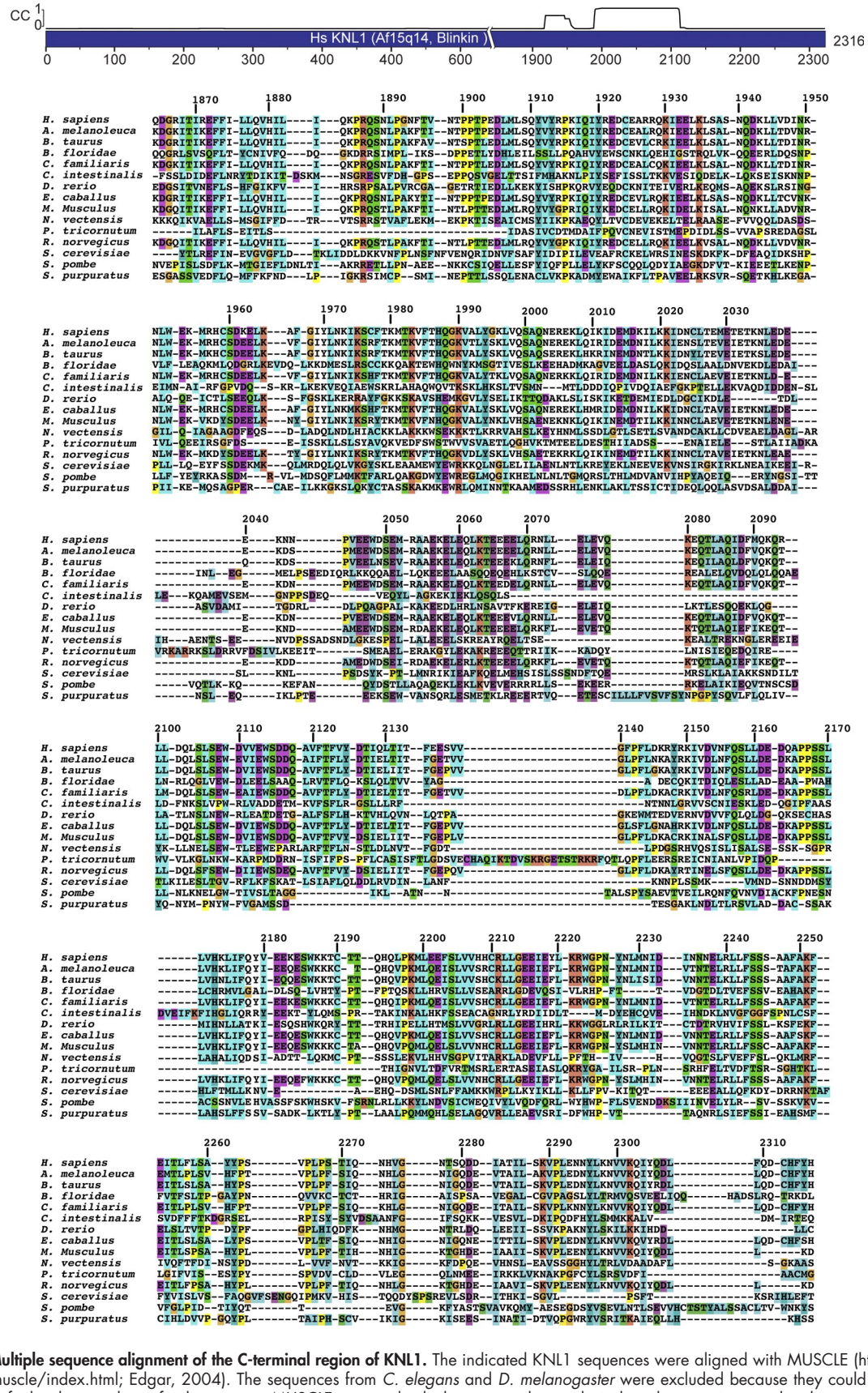

Figure S4. **Multiple sequence alignment of the C-terminal region of KNL1.** The indicated KNL1 sequences were aligned with MUSCLE (http://www.ebi.ac.uk/Tools/muscle/index.html; Edgar, 2004). The sequences from *C. elegans* and *D. melanogaster* were excluded because they could not be reliably aligned. The default coloring scheme for the program MUSCLE was used, which assigns colors exclusively to those positions in the alignment with an above-threshold level of conservation and differentiates colors based on the chemical nature of the conserved residues.

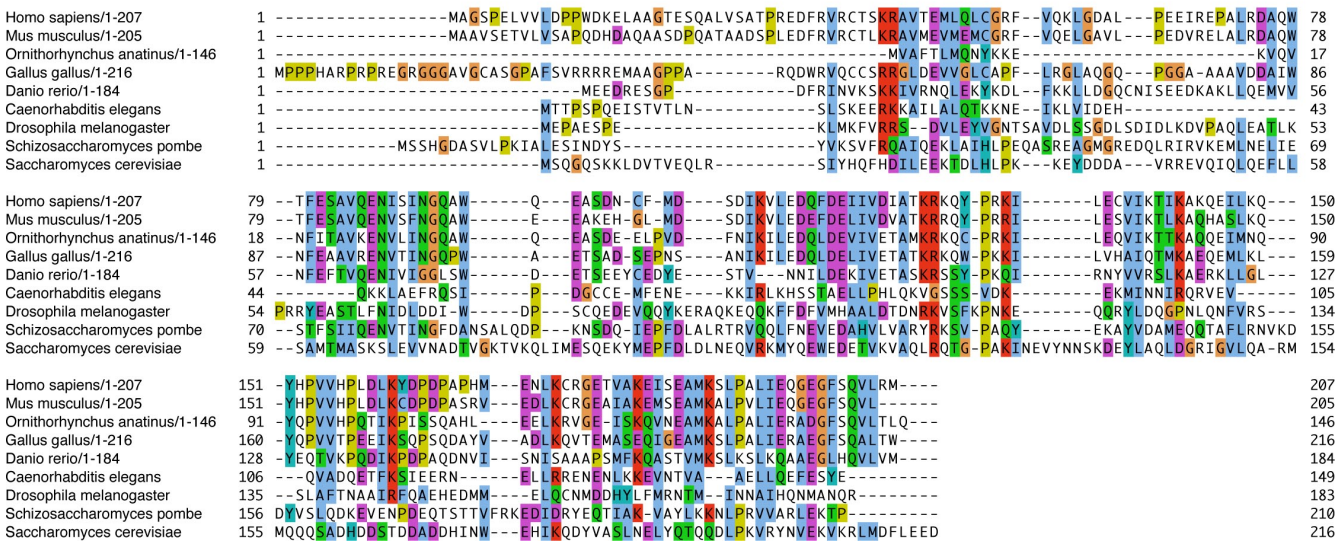

Figure S5. **Multiple sequence alignment of NSL1.** Sequences of NSL1 proteins from the indicated species were aligned with MUSCLE (Edgar, 2004). Vertebrate NSL1 proteins were aligned after removing their C-terminal region (shown instead in Fig. 2), and sequence limits of the truncated proteins are shown besides the species. The default coloring scheme for the program MUSCLE was used, which assigns colors exclusively to those positions in the alignment with an above-threshold level of conservation and differentiates colors based on the chemical nature of the conserved residues.

Table S1. **Nomenclature of KMN subunits in different species**

Complex	Subunit in indicated species				
	H. sapiens	*H. sapiens* (alternate name)	*S. cerevisiae*	*S. pombe*	*C. elegans*
KNL1C	KNL1	Blinkin/AF15q14/ CASC5/D40/	Spc105	Spc7	KNL-1
KNL1C	ZWINT	ZWINT1	YDR532c	?	KBP-5?
MIS12C[a]	MIS12	NA	Mtw1	Mis12	MIS-12
MIS12C[a]	DSN1	C20orf72/Q9H410	Dsn1	Mis13	KNL-3
MIS12C[a]	NNF1	PMF1	Nnf1	Nnf1	KBP-1
MIS12C[a]	NSL1	DC31	Nsl1	Mis14	KBP-2
NDC80C	NDC80	HEC1	Ndc80	Ndc80	NDC-80
NDC80C	NUF2	NA	Nuf2	Nuf2	JIM-10
NDC80C	SPC24	NA	Spc24	Spc24	KBP-4
NDC80C	SPC25	NA	Spc25	Spc25	KBP-3

NA, not applicable. Question marks indicate that the homologue is unknown or that the assignment of a homologue is tentative.
[a]Alias Mtw1 or MIND complex.

Table S2. **Summary of cross-linking data analysis**

Protein and start residue	Protein and end residue	Peptide 1	Peptide 2
Intramolecular sites			
DSN1, 322	DSN1, 335	VSVQLGKR	KLLK
DSN1, 61	DSN1, 335	KGGNCDLSHQER	SMQQLDPSPARKLLK
NSL1, 142	NSL1, 149	TIKAK	QEILKQYHPVVHPLDLK
PMF1, 116	PMF1, 119	IVEEGKVR	KEPAWRPSGIPEK
Intermolecular sites			
DSN1, 61	NSL1, 250	KGGNCDLSHQER	KTSDMVLKR
DSN1, 157	NSL1, 250	DTKGFSLESFR	KTSDMVLKR
DSN1, 61	NSL1, 257	KGGNCDLSHQER	KTSDMVLKR
DSN1, 335	NSL1, 268	KLLK	KWYPLRPK
DSN1, 322	NSL1, 262	VSVQLGKR	QTKDCPQR
DSN1, 157	NSL1, 257	DTKGFSLESFR	KTSDMVLKR
DSN1, 322	NSL1, 259	VSVQLGKR	KQTK
MIS12, 129	DSN1, 167	YKTELCTK	AKASSLSEELK
DSN1, 248	MIS12, 129	GSTEAKITEVK	YKTELCTK
KNL1$^{2106–2316}$, 2221	NSL1, 275	LLGEEIEYLKR	WYPLRPKK
KNL1$^{2106–2316}$, 2221	NSL1, 268	LLGEEIEYLKR	KWYPLRPK
MIS12, 200	NSL1, 142	DNVEKESKR	TIKAKQEILK

Reference

Edgar, R.C. 2004. MUSCLE: multiple sequence alignment with high accuracy and high throughput. *Nucleic Acids Res.* 32:1792–1797. doi:10.1093/nar/gkh340